J Mater Sci: Mater Med (2006) 17:1283–1296
DOI 10.1007/s10856-006-0603-y

Polyurethane/poly(hydroxyethyl methacrylate) semi-interpenetrating polymer networks for biomedical applications

L. V. Karabanova · A. W. Lloyd · S. V. Mikhalovsky · M. Helias · G. J. Phillips · S. F. Rose · L. Mikhalovska · G. Boiteux · L. M. Sergeeva · E. D. Lutsyk · A. Svyatyna

Received: 12 February 2006 / Accepted: 15 February 2006

Abstract The thermodynamic miscibility, morphology, phase distribution, mechanical properties, surface properties, water sorption, bacterial adhesion and cytotoxicity of semi-interpenetrating polymer networks (semi-IPNs) based on crosslinked polyurethane (PU) and poly(hydroxyethylmethacrylate) (PHEMA) were studied to give an insight into their structure and properties.

The free energies of mixing of the two polymers in semi-IPNs have been determined and it was shown that the values are positive and depend on the amount of PHEMA. This demonstrates that the components are immiscible, the extent of which is dependent upon variations in composition.

The morphology of the semi-IPNs was analyzed with scanning electron microscopy and tapping mode atomic force microscopy (TMAFM). The micrographs of the semi-IPNs and TMAFM phase images indicated that distinct phase separation at the nanometer scale is observed.

The mechanical properties reflect the changes in structure of semi-IPNs with composition. The stress at break increases from 3.4 MPa to 23.9 MPa, and the Young's modulus from 12.7 MPa up to 658.5 MPa with increasing amounts of PHEMA, but strain at break has a maximum at 40.4% PHEMA.

The bacterial adhesion and cytotoxicity data suggest that semi-IPNs with PHEMA content above 22% may be used for biomedical material applications.

L. V. Karabanova · L. M. Sergeeva · E. D. Lutsyk · A. Svyatyna
Institute of Macromolecular Chemistry of National Academy of Science of the Ukraine, Kharkov Road 48, Kiev 02660, Ukraine

A. W. Lloyd (✉) · S. V. Mikhalovsky · M. Helias · G. J. Phillips · S. F. Rose · L. Mikhalovska
Biomedical Materials Research Group, School of Pharmacy & Biomolecular Sciences, University of Brighton, Moulsecoomb Brighton, BN2 4GJ, UK
e-mail: a.w.lloyd@brighton.ac.uk

G. Boiteux
Laboratoire des Matériaux Polymères et Biomatériaux, UMR CNRS 5627, Université Claude Bernard Lyon 1, 15 Boulevard Latarget, 69622 Villeurbanne Cedex, France

1 Introduction

Polyurethane materials are extensively used in blood contacting applications and organ reconstruction. Although PUs are relatively biocompatible materials [1], they are also known to be prone to biodegradation [2], stress induced degradation [3] and to surface cracking [4]. Recently a lot of effort has also been focused on improving the biocompatibility of polymers used in medical implants [5, 6]. One of the most powerful approaches that can be used to improve biocompatibility and enhance the mechanical properties and resistance to degradation of polymers is to create interpenetrating polymer networks (IPNs).

Interpenetrating polymer networks are materials based on two or more polymers, each of them chemically crosslinked and at least one network synthesized in the presence of the others [7–9]. The properties of IPN materials are determined by the kinetics of formation of the growing networks and by the thermodynamics of mixing of the constituent polymers [10–12]. The miscibility of the constituent components of the IPNs is of great importance in determining the IPNs morphology [13–15]. The synthesis of IPNs is usually carried out under thermodynamically unstable conditions. This process starts from the thermodynamic equilibrium state with a mixture of the monomer(s) or polymer network swelled with a second monomer(s). During the process of polymerization, conversion of monomer to polymer results in a sharp decrease in the combinatorial entropy of mixing of the system. The result is that the Gibbs free energy of mixing of two polymers

could become positive resulting in the phase separation of the system. Many other factors play an important role in determining the properties of IPNs, including the method of synthesis, overall composition, crosslink density in both polymers, glass transition temperature and crystallinity [16–20]. As a result, IPN-based materials with improved mechanical properties [11], gas transport membranes [21] and optical gradient elements [22] can be obtained various IPN-based materials have also previously been proposed for biomedical applications [23–25]. In this study, semi-IPNs based on PU and PHEMA were synthesized and their properties investigated with a view to developing improved materials for biomedical applications by combining the mechanical properties of PU with the high biocompatibility of PHEMA.

2 Experimental

2.1 Materials

The semi-IPNs were prepared on the basis of the PU network and linear PHEMA. First the PU network was synthesized by a two step method. The first step was the preparation of the adduct of 1,1,1-trimethylolpropane (TMP) and toluylene diisocyanate (TDI). TDI was distilled under reduced pressure and TMP was dried at 308 K in vacuo. The TMP was then dissolved in ethyl acetate. The adduct of TMP and TDI was prepared by reacting 1 equivalent of TMP with 1.5 equivalents of TDI at 338 K. The reaction was carried out until the theoretical isocyanate content was reached, which was determined by the di-n-butylamine titration method. The second step was the synthesis of the cross-linked polyurethane. The polyurethane network was obtained from poly(oxypropylene)glycol ($M_w = 2000$) and the adduct of TMP and TDI (ratio 1:2 equiv.) at a temperature of 353 K in a nitrogen atmosphere over 48 h. The poly(oxypropylene)glycol was degassed at 343 K for 8 h under vacuum before use. Unreacted materials were extracted from the polyurethane network by Soxhlet extraction method using ethyl acetate as a solvent. A polyurethane network of the following structure was the desired end result:

The semi-IPNs were obtained by a sequential method, in which the polyurethane network was swollen in 2-hydroxyethyl methacrylate, freshly distilled in vacuo, containing Irgacure 651 as a photoinitiator. The swelling was carried out to the equilibrium state, and followed by the photopolymerization of the monomer in a temperature-controlled chamber for two hours. The wavelength of UV light was 340 nm.

The prepared semi-IPNs were then held in a vacuum (10^{-5} Pa) at 353 K for 36 h to reach a constant weight. A wide range of semi-IPNs with different compositions were obtained using this procedure

2.2 Vapour sorption

Methylene chloride vapour sorption by the semi-IPNs was studied using a vacuum installation and a McBain balance. The change in partial free energy of methylene chloride ($\Delta\mu_1$) by sorption (dissolution) was determined from the experimental data of methylene chloride vapour sorption by different polymer systems:

$$\Delta\mu_1 = (1/M)\, RT\, \ln(P/P_0) \tag{1}$$

where M is the molecular mass of methylene chloride and P/P_o is the relative vapor pressure. The value of $\Delta\mu_1$ changes from 0 to $-\infty$ as the weight fraction of solvent (ω_1) changes from unity to zero.

To calculate the free energy of mixing of the polymer components with solvent, it is necessary to know the changes in partial free energy of the polymers ($\Delta\mu_2$) (individual polymers or semi-IPNs).

$\Delta\mu_2$ is the difference between the polymer chemical potential in solution of a given concentration and the one in the pure polymer under the same conditions. $\Delta\mu_2$ for the polymer components have been calculated according to the Gibbs-Duhem equation for a two component system:

$$\omega_1 d(\Delta\mu_1)/d\omega_1 + \omega_2 d(\Delta\mu_2)/d\omega_1 = 0 \tag{2}$$

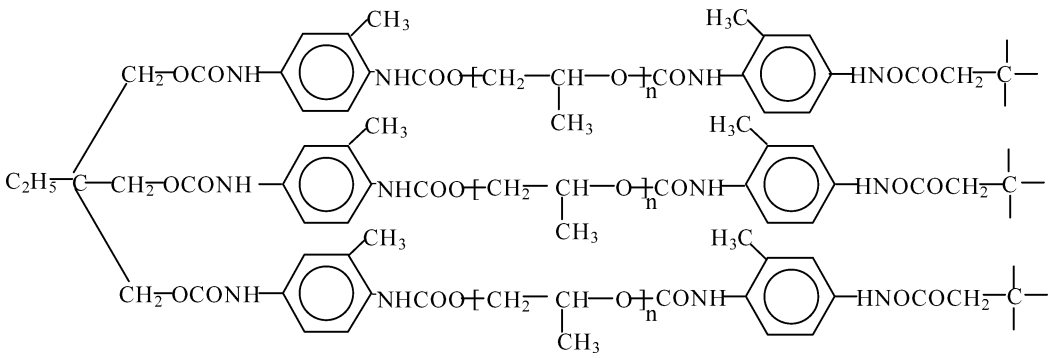

where ω_1 and ω_2 are respectively the weight fractions of the solvent and of the polymer(s).

$$\int d(\Delta\mu_2) = -\int (\omega_1/\omega_2) d(\Delta\mu_1) \quad (3)$$

Hence by integration over definite limits, the values $\Delta\mu_2$ can be found from the experimental data.

The average free energy of mixing Δg^m of the solvent with individual polymers or semi-IPNs of various compositions for solutions of different concentrations, was estimated according to the equation:

$$\Delta g^m = \omega_1 \Delta\mu_1 + \omega_2 \Delta\mu_2 \quad (4)$$

2.3 Morphological analysis

Electron micrographs were obtained using a JEOL JSM 6310 scanning electron microscope (SEM). Samples of the semi-IPNs were fractured in liquid nitrogen and chemically treated with aqueous I_2 and KI. They were then freeze-dried overnight before being examined by electron microscopy. After drying the specimens were sputter coated with gold to avoid electrostatic charges and to improve image resolution. For the best representation, the whole sample area was examined before representative micrographs were taken.

2.4 Atomic force microscopy

Surface topography and phase images were obtained using a multimode Nanoscope IIIa atomic force microscope. Tapping mode was employed in air using a 125 μm silicon tip. Topographic and phase images were obtained simultaneously.

2.5 Mechanical testing

The mechanical properties of the semi-IPNs were measured using a Series IX Automated Instron Materials Testing System. The samples were cut into micro dumb-bell shapes with a gauge length of 20 mm, widths between 2–5 mm, and sample thickness between 0.7–0.9 mm. Samples were elongated at a continuous strain rate of 25 mm/min. The mechanical properties of the semi-IPNs were measured for samples in a dry state and for samples in a hydrated state following 48 h in water.

2.6 Surface properties

The surface properties of semi-IPNs have been investigated using a Cahn 322 dynamic contact angle analyser and WinDCA software.

2.7 Sorption of water

The sorption of water by the samples of PU, PHEMA and the semi-IPNs was measured by a weight method at 25°C under equilibrium conditions.

2.8 Bacterial adhesion

The adhesion of *Staphylococcus aureus* 10788 (NCTC) to the surface of the samples was used to assess bacterial adhesion of the semi-IPNs. Sample materials were cut into 1 cm^2 pieces and sterilised under UV before incubating with 1 ml of bacteria at 1×10^8 cells/ml. Samples were incubated with the bacteria for 4 h at 37°C, shaking at 120 rpm. Adhesion of *S. aureus* was assessed by quantifying the amount of ATP released from the adherent cells using a Vialight microbial detection kit (BioWhittaker UK Ltd.); ATP was released from the bacterial cells after incubation in a lysis buffer (Bactolyse) for 15 min at room temperature and then detected using a 96 well plate luminometer (Anthos Lucy I) after addition of ATP monitoring reagent. The number of adherent bacterial cells per sample was calculated against a standard curve of known bacterial concentrations.

2.9 Cytotoxicity of the semi-IPNs

The cytotoxicity of the semi-IPNs was investigated to assess the effect of material leachate on mammalian cells in order to determine the viability of these materials for use as biomaterials. Cytotoxicity was evaluated using a colony formation assay [ISO/TC194; Japanese guidelines for basic biological tests of medical materials and devices]. Each sample material (0.4 g) was UV sterilised and cut into small pieces ($\sim 2 \times 5$ mm). Each sample was then incubated with 4 ml of Dulbecco's Modified Eagle's Medium (DMEM, Invitrogen) supplemented with 5% foetal calf serum (FCS) and 1% penicillin and streptomycin for 24 h in a cell culture incubator set at 37°C and 5% CO_2. V79 cells, maintained in the above supplemented media were seeded at 50 cells per well in 24 well tissue culture plates and incubated for 24 h in a cell culture incubator. After incubation the material extracts were diluted in media to 100, 50, 25, 12.5, 6.3, 3.1, 1.6 and 0% of the original extract. After 24 h the media was removed from the cells and 0.5 ml of each dilution was added to the wells (3 replicate wells per sample dilution). The plates were then incubated for a further 5 days. The resulting cell colonies were fixed in methanol and stained with 10% Giemsa stain. The colonies were then counted and the average number for each dilution and sample type was calculated. The cytotoxicity of each material type was determined by the reduction in colony formation compared to the control wells (0% extract) and

the EC50% values (the extract concentration which reduced colony formation by 50%) calculated.

3 Results and discussion

3.1 Miscibility of the semi-IPNs

Previous studies have shown that microphase separation is typical for IPNs and semi-IPNs, and that the systems have a "frozen" non-equilibrium structure [10, 11, 16, 17]. This non-equilibrium structure is the result of two processes: the chemical reaction of the IPNs formation and the physical process of microphase separation accompanying the reaction. The optical transparency of the resulting semi-IPNs is not sufficient evidence to allow firm conclusions to be drawn regarding the miscibility of the polymer components. To estimate the thermodynamic state of the semi-IPNs we calculated the free energy of mixing of the constituent polymers. For this purpose we have studied the sorption of methylene chloride vapour by all the samples under investigation. Figure 1 demonstrates sorption isotherms of methylene chloride at 20°C by PU (1), PHEMA (2) and semi-IPNs of various compositions (3–8). The isotherm of PU (1) has a shape typical of an elastomer. For PHEMA (2), the sorption of methylene chloride is very small in the range of the relative pressures up to 0.4, then it increases. This behaviour is typical of glassy state polymers [26]. At a relative pressure of methylene chloride in the region of 0.4, the amount of solvent in the sample of PHEMA is enough to allow the transition of the polymer from a glassy state to an elastic state. From this point the sorption of the solvent by the PHEMA increases. The behaviour of the semi-IPNs (Fig. 1, curves 3–8) lies between the two extremes for the individual constituent polymers.

The thermodynamic parameters were calculated from the methylene chloride vapour sorption data using the method described earlier. In Fig. 2, the change of the free energy of mixing of methylene chloride with individual PU (curve 1), with PHEMA (curve 2) and with semi-IPNs (curves 3–8) is shown. It is evident that all the systems studied (PU—methylene chloride, PHEMA—methylene chloride

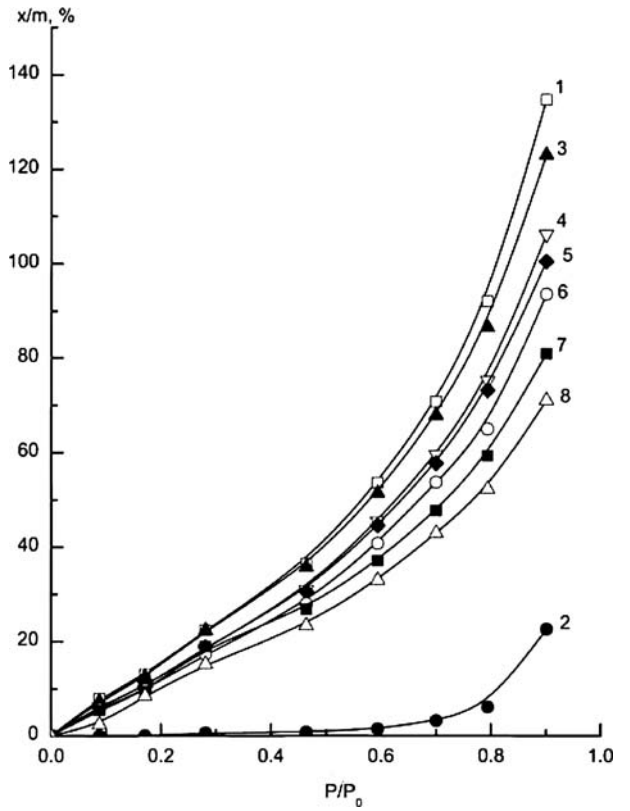

Fig. 1 Sorption isotherms of methylene chloride vapour by Polyurethane (1), poly(hydroxyethyl methacrylate) (2), semi-IPNs with 10.72% (3), 16.15% (4), 21.40% (5), 31.89% (6), 40.35% (7) and 57.48% (8) of poly(hydroxyethyl methacrylate). x/m–wt% methylene chloride sorped per gram of dry sample; P/P_o-relative pressure of methylene chloride

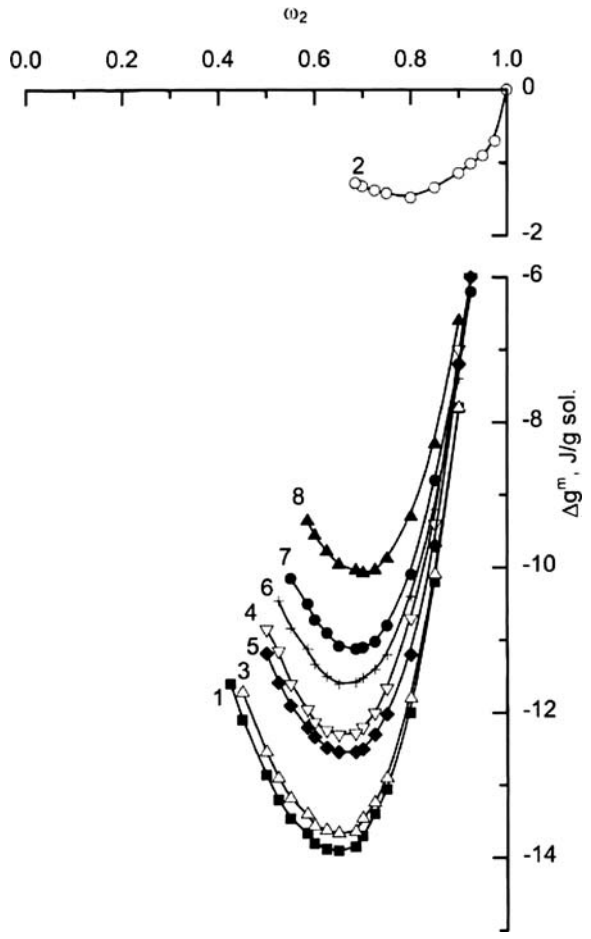

Fig. 2 Free energy of mixing Δg^m versus weight fraction of polymer (semi-IPNs) ω^2 with solvent: (1) PU, poly(hydroxyethyl methacrylate) (2), semi-IPNs with 10.72% (3), 16.15% (4), 21.40% (5), 31.89% (6), 40.35% (7) and 57.48% (8) of poly(hydroxyethyl methacrylate)

Table 1 Variation of the free energy of mixing (Δg^m) of polyurethane and poly(hydroxyethylmethacrylate) in semi-IPNs

Composition of semi-IPN	Δg^m ($J \cdot g^{-1}$)
Semi-IPN with 10.72% PHEMA	+0.20
Semi-IPN with 16.15% PHEMA	+0.35
Semi-IPN with 21.40% PHEMA	+0.40
Semi-IPN with 31.89% PHEMA	+0.50
Semi-IPN with 40.35% PHEMA	+1.20
Semi-IPN with 57.48% PHEMA	+2.75

and semi-IPNs- methylene chloride) are thermodynamically stable ($d^2\Delta g^m/d\omega_2^2 > 0$). There is a great difference between the affinity of methylene chloride for PU and for PHEMA and this affinity is lower in the case of the methylene chloride-PHEMA system (Fig. 2, curve 2) than for methylene chloride-polyurethane (Fig. 2, curve 1). The affinity of methylene chloride for the semi-IPNs rises as the amount of PU in the samples increases (Fig. 2, curves 3–8).

From the concentration dependence of the free energy of mixing of methylene chloride and the system components (Fig. 2), using the thermodynamic cycles [26], we have calculated the changes in free energy of mixing between the PU and PHEMA in semi-IPNs with a wide range of compositions. The data are presented in Table 1.

From the data shown in Table 1 it is evident that the values of the free energy of mixing are positive. This demonstrates that the components are immiscible, the whole semi-IPN being thermodynamically unstable. Thermodynamic stability of these semi-IPNs cannot be reached due to the network of PU which prevents further full phase separation. This suggests that complete phase separation of the immiscible polymer components of semi-IPN did not occur, the process of phase separation being prevented by the PU network formation.

3.2 Mechanical behaviour

The mechanical behaviour of semi-IPN samples was examined both in a dry state and a hydrated state. The stress-strain curves for the dry samples (Fig. 3(a) and (b)), are the median curves for six studies made with each semi-IPN sample. They indicate that the ultimate strength increased with increasing PHEMA content in semi-IPNs. At the same time the strain at break also increased with increasing the PHEMA content up to 40.4%. For the last sample, with a PHEMA content of 57.7%, the strain at break decreased sharply with an increase in the stress at break. The curve for PU (Fig. 3(a), curve 1) is typical of elastomers [27]. The same type of stress-strain curve is observed for semi-IPNs with a PHEMA content of 6.6–40.4% (Fig. 3(a) and (b), curves 2–7). This could signify that PU forms a continuous phase in these samples. The mechanical properties of the semi-IPNs change with increasing PHEMA content up to 57.7% (Fig. 3(b), curve 8). Firstly, the shape of curve changed significantly. This material demonstrated ductility, and the stress at break increased sharply in comparison with the previous samples. The stress-strain curve of the semi-IPN containing 57.7% PHEMA is typical of amorphous glassy polymers containing an elastomeric phase as a filler [27]. This could suggest that in semi-IPNs containing 57.7% PHEMA, the PHEMA forms a second continuous phase.

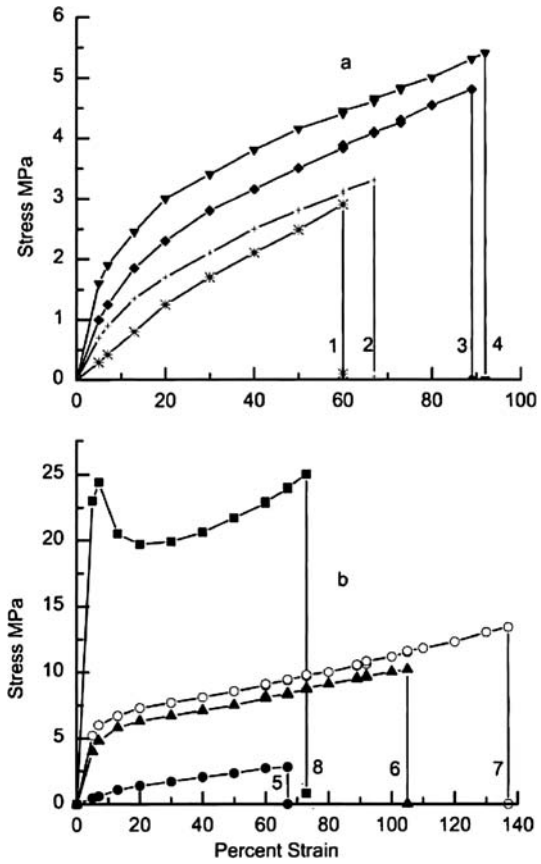

Fig. 3 Stress-strain curves of semi-IPN films: (a) PU (1); 6.6% PHEMA (2); 10.7 % PHEMA (3); 16.2% PHEMA (4); 21.4% PHEMA (5); (b) 31.9% PHEMA (6), 40.4% PHEMA (7); 57.7% PHEMA (8)

The mechanical properties of semi-IPNs are given in more details in Table 2. The data reflect changes in the structure of semi-IPNs with increasing amounts of PHEMA in the system. The strain at break has a maximum at 40.4% of PHEMA. The stress at break increases from 3.4 MPa to 23.9 MPa with increasing PHEMA content in the semi-IPNs (Table 2). It is important to note that the Young's modulus increases from 7.6 MPa up to 658.5 MPa with increasing PHEMA content in the samples. Moreover, the Young's modulus increases sharply from 157.3 MPa to 658.5 MPa as the amount of PHEMA increases from 40.3% to 57.7%. This evidence supports the notion of a second continuous phase in semi-IPNs containing 57.7% PHEMA.

Table 2 Mechanical properties of the semi-interpenetrating polymer networks based on Polyurethane and Poly(hydroxyethyl methacrylate)

Sample	Strain at peak (%)	Stress at peak (MPa)	Strain at break (%)	Stress at break (MPa)	Young's Modulus (MPa)
PU	56.8	2.5	58.2	2.4	7.7
Semi-IPN 6.6% PHEMA	82.6	3.4	83.3	3.4	12.7
Semi-IPN 10.7% PHEMA	64.2	3.3	64.7	3.0	16.8
Semi-IPN 16.2% PHEMA	96.2	5.1	96.8	5.0	26.2
Semi-IPN 21.4% PHEMA	100.2	5.6	100.8	5.1	42.9
Semi-IPN 31.9% PHEMA	136.8	9.9	137.6	9.8	65.0
Semi-IPN 40.4% PHEMA	141.4	13.7	141.7	13.7	157.3
Semi-IPN 57.7% PHEMA	76.6	26.4	78.6	23.9	658.5

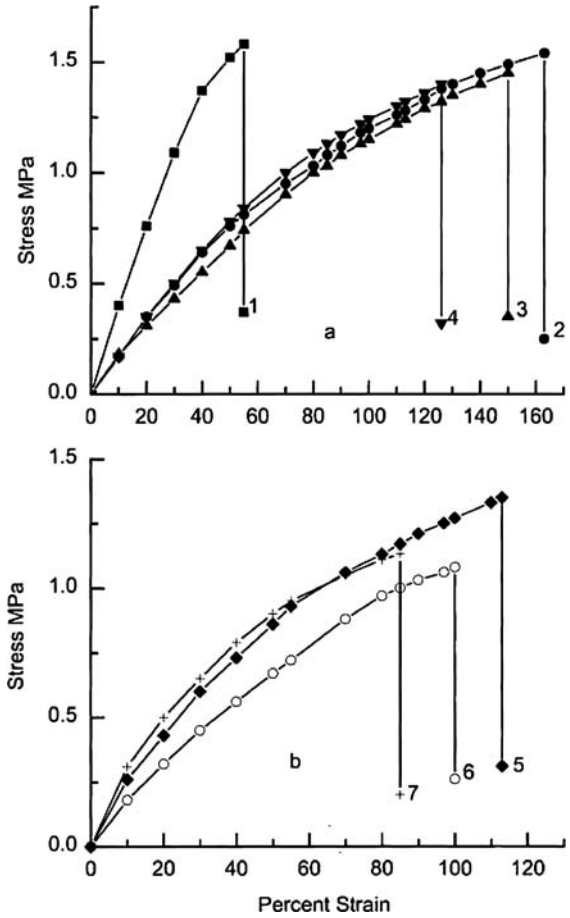

Fig. 4 Stress-strain curves of semi-IPN films after 48 h conditioning in water: (a) PU (1), 10.72% PHEMA (2), 16.15% PHEMA (3), 21.40% PHEMA (4), (b) 31.89% PHEMA (5), 40.35% PHEMA (6), 57.70% PHEMA (7)

It is important to understand the mechanical properties of materials in their hydrated state if they are intended for use in bioengineering applications and implantation into the body. The mechanical behaviour of semi-IPNs was therefore examined in samples that were swollen in water for 48 h prior to testing. The results are presented in Fig. 4. The curve for PU in its hydrated state (Fig. 4(a), curve 1) did not change greatly in comparison with the dry sample (Fig. 3(a), curve 1). The same type of stress-strain curve is observed for all hydrated semi-IPNs with a PHEMA content in the range 6.6–57.7% (Fig. 4(a) and (b), curves 2–8). This type of stress-strain curve is typical for elastomers, suggesting transition of swollen PHEMA from a glassy to elastic state.

The strain at break for samples of semi-IPNs in a hydrated state increased in comparison with samples in dry state. However, the ultimate strength of samples in a hydrated state sharply decreased, with all samples demonstrating an ultimate strength of between 1 MPa and 1.5 MPa (Fig. 4). This demonstrates that the mechanical behaviour of semi-IPNs in their hydrated state is mainly governed by the PU's behaviour. Therefore, hydrated semi-IPNs based on PU and PHEMA retain their mechanical properties to a level appropriate for use for bioengineering applications.

3.3 Sorption of water by semi-IPNs

Although PHEMA displays good biocompatibility, allegedly due to its hydrophilicity, it is a hygroscopic material and its mechanical properties are affected by atmospheric humidity. The synthesis of semi-IPNs based on PU and PHEMA offers a means of overcoming such limitations. The sorption kinetics of water vapour by the samples of PU, PHEMA and semi-IPNs at 25°C and 100% relative humidity are shown in Fig. 5. Sorption of water by PU is low, being only 2 wt% compared to that for pure PHEMA (32% wt%). For the semi-IPNs, the sorption of water increased from 4% to 21.5% as the PHEMA content increased from 6.6% to 57.7%. The reduced water sorption at equilibrium led to improved mechanical properties of the IPNs when compared to PHEMA alone and allowed preservation of the mechanical properties of hydrated semi-IPNs to a tolerable level (Fig. 4).

3.4 Surface properties of semi-IPNs

Despite the extraordinary versatility of polymers, there is one property that markedly limits their medical applications, and that is surface hydrophobicity. It makes the typical polymer difficult to wet, coat and adhere. With surface energies lower than in most materials, polymers are often incompatible with

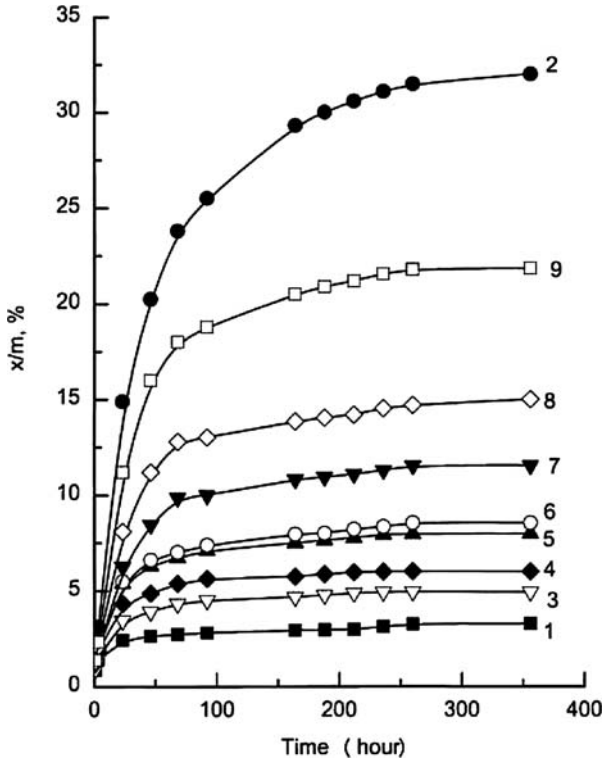

Fig. 5 Sorption of water vapour by PU (1), PHEMA (2) and their semi-IPNs with 6.6% (3), 10.7% (4), 16.2% (5), 21.% (6), 31.% (7), 40.% (8) and 57.% (9) of PHEMA

other higher energy materials. When placed in a relatively hydrophilic environment such as the human body, these polymers may be rejected. Any improvement in the hydrophilicity of hydrophobic polymers could lead to their better biocompatibility.

The surface properties of semi-IPNs were investigated using dynamic contact angle analysis. The advancing contact angle at the air-water interface for the semi-IPNs changes in a non-monotonic way with maximum at low PHEMA contents in the semi-IPNs (Table 3). With increasing PHEMA content, the advancing contact angle gradually decreases. The same regularity could be seen for the receding contact angle (Table 3). Contact angle hysteresis is well known and may be due to a number of factors including molecular reorganisation at the surface [28]. In this complex system it is also possible that the variation in contact angle could be attributed to the changes in the microrugosity of the surface caused by differences in the primary phases domains at the surface (see below). Although it is difficult to make any direct correlation between the biocompatibility of the material and its surface properties, this increased surface hydrophilicity may result in improved biocompatibility of semi-IPNs with vascular tissues [29–31].

Table 3 Variation of the dynamic contact angle in the semi-IPNs based on polyurethane and poly(hydroxyethyl methacrylate)

PHEMA (wt%)	Advancing contact angle	Receding contact angle
0 (PU)	78.3	53.0
6.6	92.1	58.6
10.7	93.7	60.2
16.2	77.4	54.0
31.9	72.8	21.2
40.4	75.0	39.1
57.7	69.3	16.1
100	90.7	29.5

3.5 Morphology of semi-IPNs

The 1-mm-thick PU, PHEMA and semi-IPNs sheets were visually transparent although the thermodynamic studies indicated that PU and PHEMA are immiscible in these semi-IPNs. This could signify that PHEMA domains in PU matrix are smaller than the wavelength of visible light. Scanning electron microscopy was therefore used to investigate the details of the semi-IPNs morphology (Figs. 6 and 7). The pure PU network (Fig. 6(a) and (b)) demonstrated the segregation of hard and soft segments within the PU. The micrograph of PHEMA (Fig. 6(c) and (d)) revealed a smooth structure. The semi-IPNs, however, demonstrated complicated domain structures indicating phase separation in the nanoscale size range (Fig. 6(f) and (h); Fig. 7(b), (f) and (h)). With increasing PHEMA content, up to concentration of 21.4%, separate small domains of PHEMA in the PU matrix were observed (Fig. 6 (f) and (h); Fig. 7(b)). The brittle failure of semi-IPNs above 21.4% PHEMA demonstrated significant changes in structure in these materials in comparison to the previous samples (Fig. 7(c), (e) and (g)). At this point the micrographs demonstrated smoother structures (Fig. 7(d), (f) and (h)), suggesting the appearance of a bicontinuous phase structure in semi-IPNs containing greater than 21.4% PHEMA. Finally, the micrograph for the semi-IPN with 57.7% PHEMA showed that an inversion of phases occurred (Fig 7(g) and (h)) with PHEMA becoming a matrix containing phase domains of PU. These results are in agreement with the changes in the mechanical properties of the semi-IPNs: above 40.4% PHEMA the stress-strain curve of semi-IPNs also changed significantly (Fig. 3(b), curve 8).

3.6 Atomic force microscopy

Phase imaging is a powerful extension of tapping mode atomic force microscopy that provides nanometre scale information about surface structure not revealed by other techniques. Phase imaging goes beyond simple topographical mapping to detect variations in composition, viscoelasticity, adhesion and other properties. This technique allows the

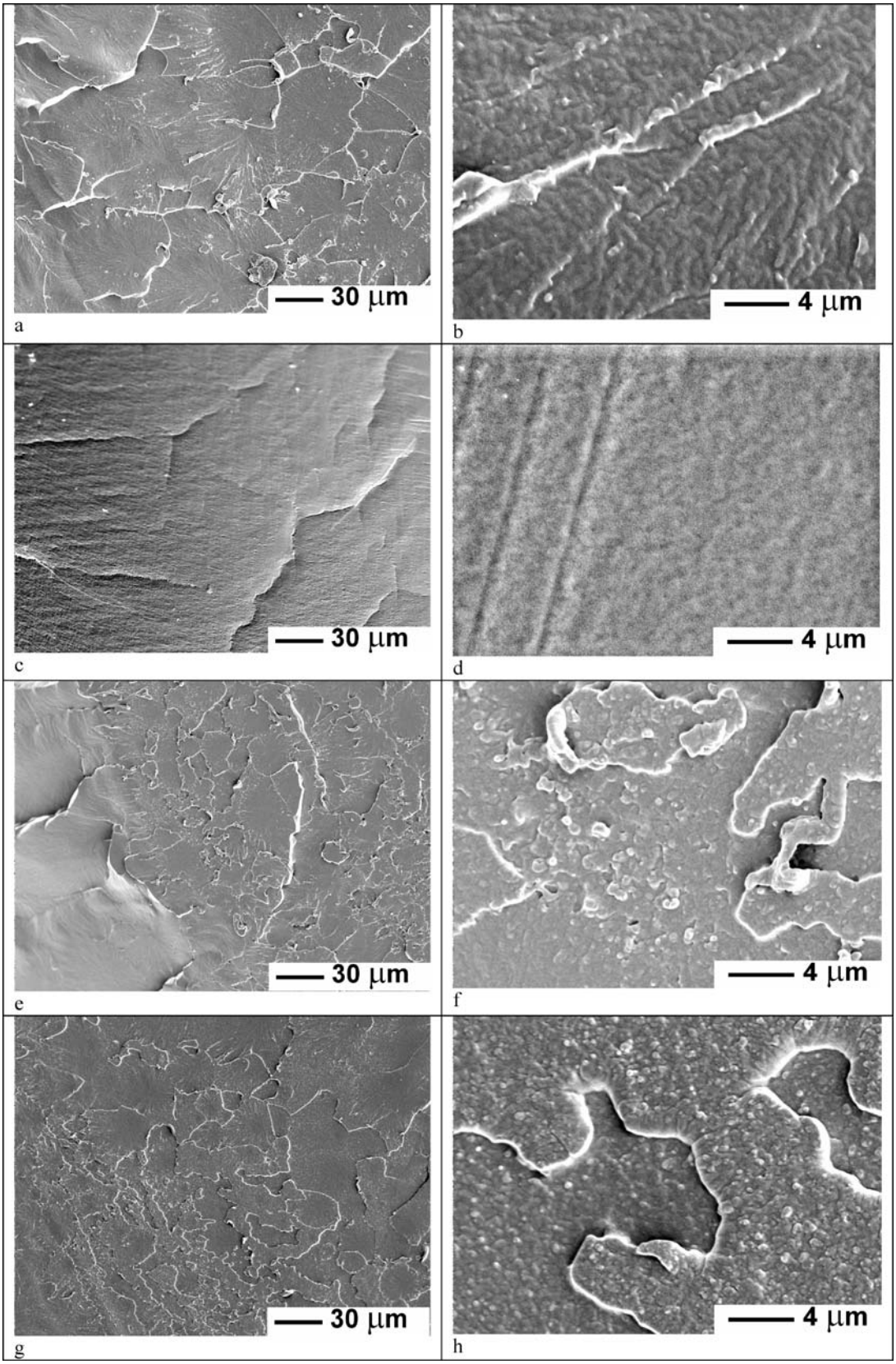

Fig. 6 Scanning electron micrographs of different semi-IPNs based on PU and PHEMA: (a) and (b) pure PU, (c) and (d) pure PHEMA, (e) and (f) 10.7% PHEMA, (g) and (h) 16.2% PHEMA

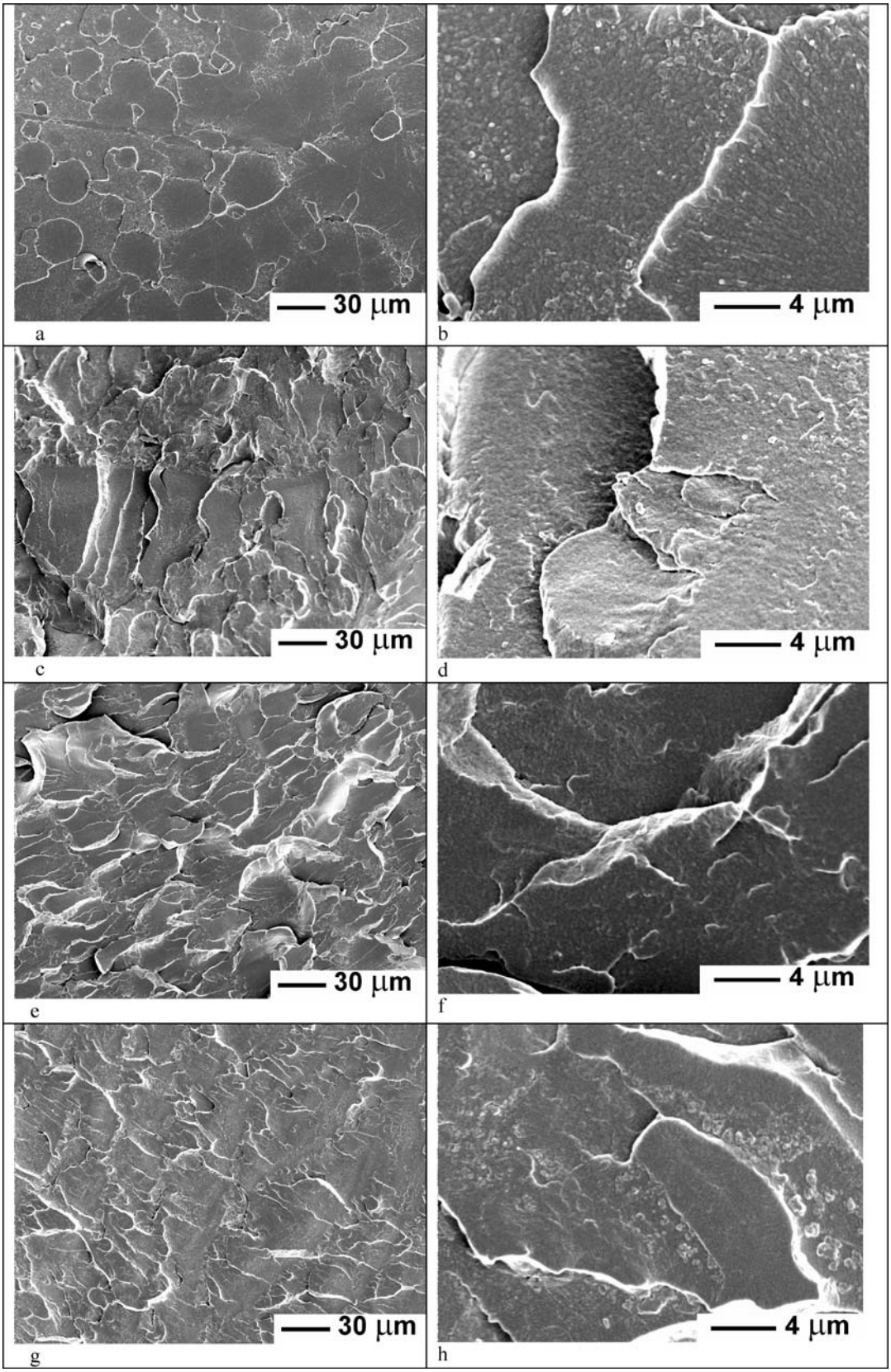

Fig. 7 Scanning electron micrographs of semi-IPNs based on PU and PHEMA: (a) and (b) 21.4% PHEMA, (c) and (d) 31.9% PHEMA, (e) and (f) 40.4% PHEMA, (g) and (h) 57.7% PHEMA

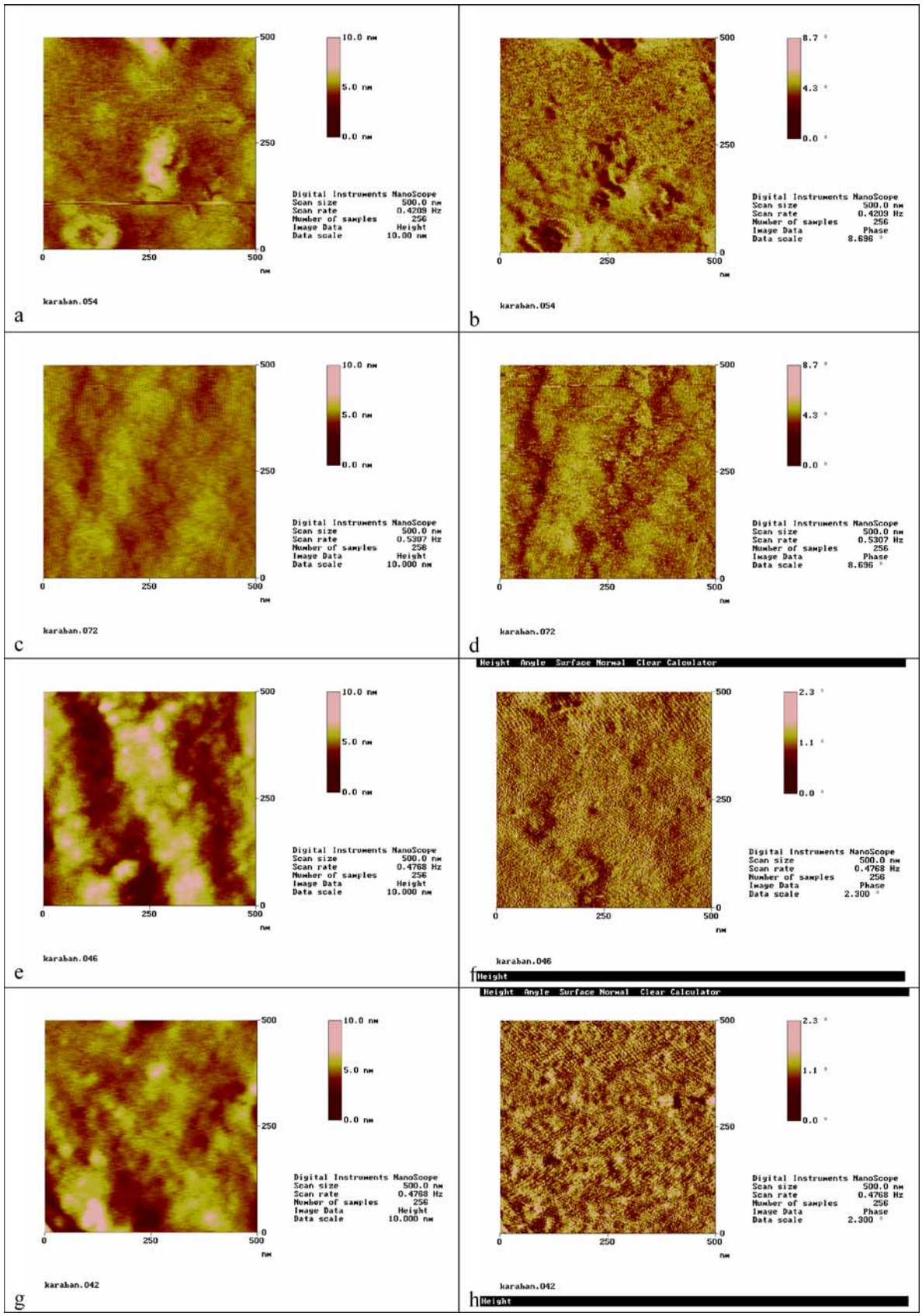

Fig. 8 Tapping mode AFM topography (left) and phase images (right) for the various polymers: PU (a, b); PHEMA (c, d); 10.72% PHEMA (e, f) and 16.15% PHEMA (g, h)

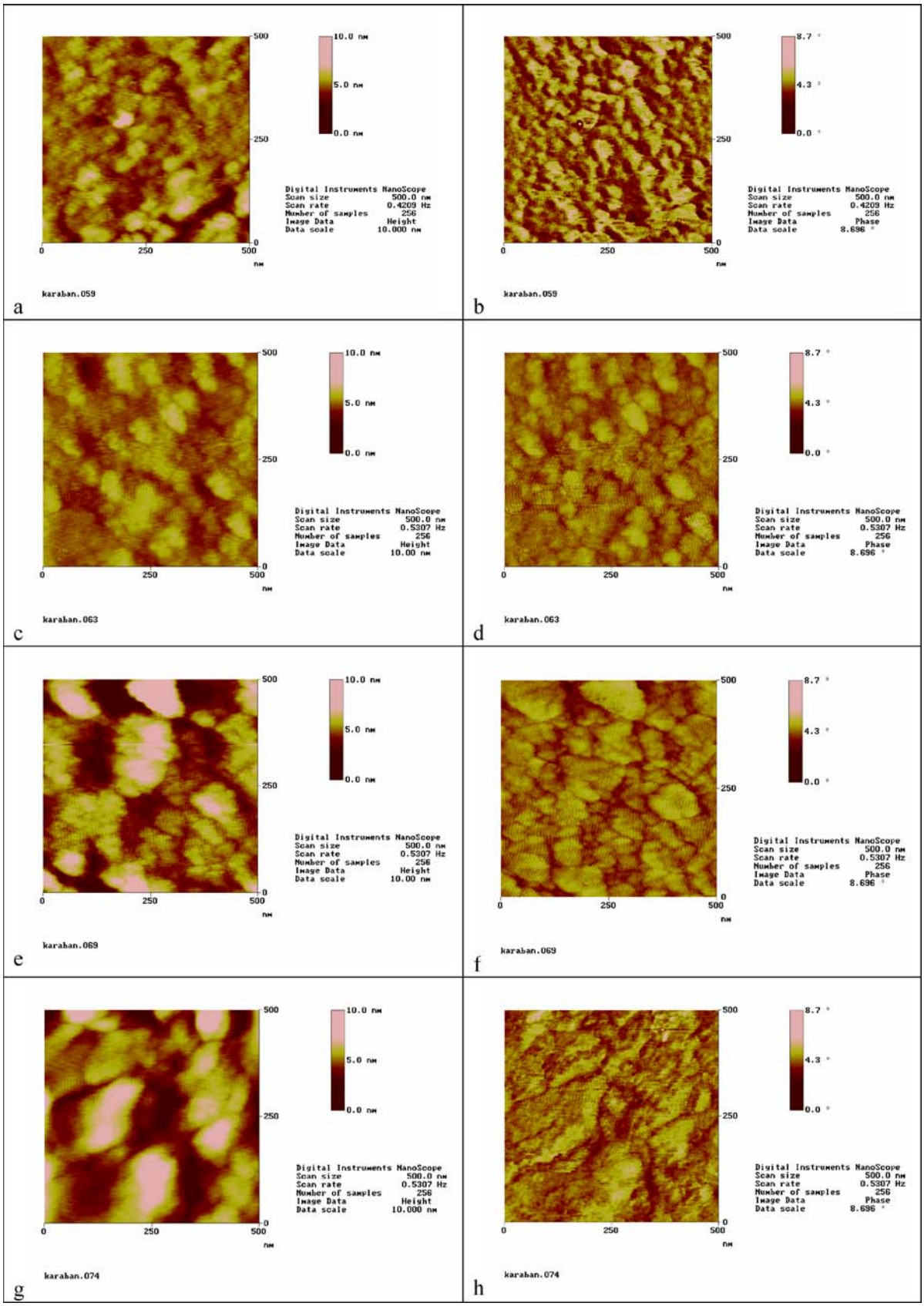

Fig. 9 Tapping mode AFM topography (left) and phase images (right) for the various polymers: 21.40% PHEMA (a, b); 31.89% PHEMA (c, d); 40.35% PHEMA (e, f); 57.70% PHEMA (g, h)

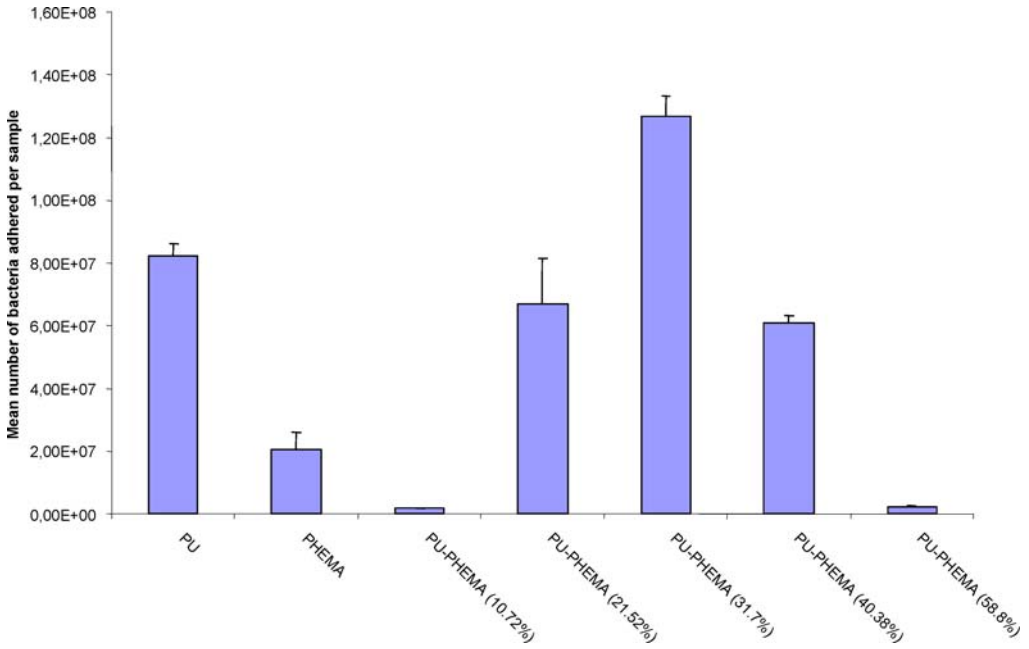

Fig. 10 *Staphylococcus aureus* adhesion to PU, PHEMA and the semi-IPN materials (Mean ± sd, $n = 6$–9)

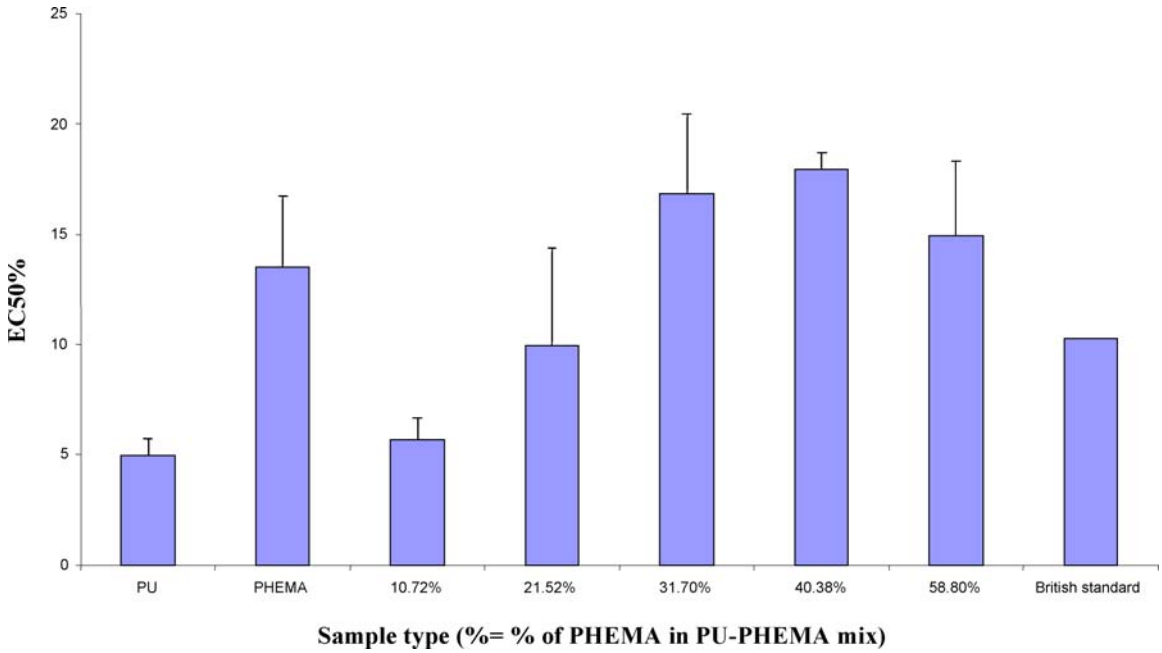

Fig. 11 Cytotoxicity of PU, PHEMA and semi-IPN materials. The EC_{50} is the extract concentration which reduced colony formation by 50% (mean ± SD, n = 3). British standard (PVC containing 0.57% dibutyl tin dimaleate (Portex Ltd, UK)) material was used as an internal control material.

identification of different components in composite materials, and different regions of high and low surface adhesion or hardness at very high resolution.

Phase and topography images of PU and PHEMA semi IPNs are presented in Figs. 8 and 9. Pure PU demonstrated the segregation of hard and soft segments (Fig. 8(a) and (b)). Pure PHEMA displays no phase separation with the surface of the sample appearing homogeneous and flat (Fig. 8(c) and (d)). In the semi-IPNs a distinct phase separation is observed at the nanometer scale (Fig. 8(e) and (f), (g) and (h); Fig. 9(a)–(h)). Phase domains of 15–25 nm could be observed in the semi-IPNs with a PHEMA content of 10.72–16.15%. With increasing amounts of PHEMA in the semi-IPNs up to 40.35%, the size of the domains increased to 25–50 nm

(Fig. 9(a)–(f)). A bi-continuous phase structure could be observed in the semi-IPN with 57.7% PHEMA (Fig. 9(g) and (h)) and an inversion of phases could be seen.

3.7 Bacterial adhesion

The adhesion of *S. aureus* 10788 (NCTC) may be used as a preliminary test of microbial adherence to polymers. Bacterial adhesion to samples of PU and semi-IPNs based on PU and PHEMA are shown in Fig. 10. Although the adhesion of *S. aureus* to PU is four times grater than that to PHEMA, the dependence of bacterial adhesion on the PHEMA content in the semi-IPNs is complex and may be related to the changes in the microstructure on the surface of the material. Taking into account that the mechanical properties of the PU-PHEMA semi-IPNs are improved compared to pure PU (Figs. 3 and (4)), and that the semi-IPNs with PHEMA content above 22% are less toxic (Fig. 11), this result suggests that semi-IPN compositions containing 22, 40 and 58% PHEMA have optimised characteristics for use as biomedical materials.

3.8 Cytotoxicity of the semi-IPNs materials

The cytotoxicity of extracts from the semi-IPN samples was determined using a mammalian cell colony forming assay. The concentration of extracts from the semi-IPN samples needed to reduce colony formation by 50% is shown in Fig. 11. It is clear from the data shown that PHEMA is less toxic than PU. For semi-IPNs the cytotoxicity decreases with increasing amounts of PHEMA in the samples. In comparison with the British Standard, which is also presented in Fig. 11, the semi-IPN samples with a concentration of PHEMA above 22% show reduced toxicity. This means that semi-IPNs based on PU and PHEMA could be used for bioengineering purposes.

4 Conclusions

The thermodynamic miscibility, morphology, phase distribution, mechanical properties, surface properties, water sorption, bacterial adhesion and cytotoxicity of semi-interpenetrating polymer networks based on cross-linked PU and PHEMA have been investigated. The free energies of mixing of the semi-IPN components are positive and depend on the amount of PHEMA in the semi-IPN samples, demonstrating that the components are immiscible. The different levels of immiscibility in the semi-IPNs are related to the variations in composition. The morphological investigations show that the semi-IPNs have complicated domain structures indicating phase separation at the nanoscale size range. A bi-continuous phase structure appeared in the semi-IPNs above 21.4% PHEMA. Finally, an inversion of phases occurred in the semi-IPN with 57.7% PHEMA, with PHEMA becoming the primary matrix in the semi-IPN of this composition. These results suggest that the studied semi-IPNs are two-phase systems with incomplete phase separation. The results of the morphological investigations concur with mechanical properties of the semi-IPNs. Above 40.3% PHEMA a marked change is observed in the stress-strain curves of the materials. The mechanical properties reflect the changes in structure of semi-IPNs with increasing PHEMA content in the system. The stress at break changes from 3.4 MPa to 23.9 MPa with increasing PHEMA content in the semi-IPNs, but strain at break has a maximum at 40.4% PHEMA. It is important to note that Young's modulus increases from 12.7 MPa up to 658.5 MPa with increasing PHEMA content. The bacterial adhesion and cytotoxicity data suggest that the semi-IPNs with PHEMA content of 22, 40 and 58% may be used for biomedical material applications.

Acknowledgments L. Karabanova gratefully acknowledges the Royal Society of UK for financial support and thanks the members of the Biomedical Materials Research Group of the School of Pharmacy & Biomolecular Sciences, University of Brighton for their hospitality and support during her exchange visit.

References

1. M. D. LEHAH and S. L. COOPER, in "Polyurethane in Medicine and Surgery" (CRC Press, Boca Raton, FL, 1986) p. 158.
2. R. W. PAYNTER, H. MARTZ and R. GUIDOIN, *Biomaterials* **94** (1987) 8.
3. R. J. THOMA, *J. Biomater. Appl.* **449** (1987) 1.
4. M. SZYCHER, D. DEMPSEY and V. L. POIRIER, *Trans. Am. Soc. Biomater.* **24** (1984) 7.
5. A. W. LLOYD, R. G. A. FARAGHER and S. P. DENYER, *Biomaterials* **769** (2001) 22.
6. A. B. LOWE, M. VAMVAKAKI, M. A. WASSALL, L. WONG, N. C. BILLINGHAM, S. P. ARMES and A. W. LLOYD, *J. Biomed. Mat. Res.* **88** (2000) 52.
7. L. H. SPERLING and V. MISRA, in "IPNs Around the World: Science and Engineering," edited by S. C. Kim and L. H. Sperling (Wiley, 1997) p. 16.
8. V. D. ATHAWALE, S. L. KOLEKAR and S. S. RAUT, *J. Macromol. Sci., Part C–Polym Rev.* **43** (2003) 1.
9. L. H. SPERLING and R. HU, in "Polymer Blends Handbook," edited by L. A. Utracki (Kluwer, Dordrecht, 2002) p. 56.
10. YU. S. LIPATOV, in "Polymer Reinforcement" (Chem. Tec. Publ., Ontario, 1995) p. 286.
11. Y. S. LIPATOV and L. V. KARABANOVA, in "Advances in Interpenetrating Polymer Networks" (Technomic Publ. Company, Inc., Lancaster, 1994) p. 191.
12. Y. S. LIPATOV, in "Advances in Interpenetrating Polymer Networks," edited by D. Klempner and K. Frisch (Technomic Publ. Company, Inc., Lancaster, 1989) p. 261.
13. L. V. KARABANOVA, P. PISSIS, A. KANAPITSAS and E. D. LUTSYK, *J. Appl. Polym. Sci.* **68** (1998) 161.
14. Y. S. LIPATOV, L. V. KARABANOVA and L. M. SERGEEVA, *Polym. Intern.* **34** (1994) 7.
15. Y. S. LIPATOV, G. M. SEMENOVICH, S. I. SKIBA, L. V. KARABANOVA and L. M. SERGEEVA, *Polymer* **33** (1992) 361.

16. Y. S. LIPATOV, *J. Macromol. Sci. Rev. Macromol. Chem. Phys.* **C30** (1990) 209.
17. Y. S. LIPATOV, L. V. KARABANOVA, L. A. GORBACH, E. D. LUTSYK and L. M. SERGEEVA, *Polym. Intern.* **28** (1992) 99.
18. L. V. KARABANOVA, G. BOITEUX, O. GAIN, G. SEYTRE, L. M. SERGEEVA and E. D. LUTSYK, *J. Appl. Pol. Sci.* **80** (2001) 852.
19. J.-M. WIDMAIER and G. C. MEYER, in "Advances in Interpenetrating Polymer Networks," edited by D. Klemper and K. Frisch (Technomic Publ. Company, Inc., Lancaster, 1989) Vol. 1, p. 155.
20. X. M. XU, H. TOGHIANI and C. U. PITTMAN, *Polym. Eng. Sci.* **40** (2000) 2027.
21. K. H. HSIEH, C. C. TSAI and S. M. TSENG, *J. Membr. Sci.* **341** (1990) 49.
22. Y. OHTSUKA, *Appl. Phys.* **247** (1973) 23.
23. M. DROR, M. Z. ELSABEE and G. C. BERRY, *Biomater. Med. Devices Artif. Organs* **14** (1979) 7.
24. P. PREDECKI, *J. Biomed. Mater. Res.* **487** (1974) 8.
25. P. D. NAIR and V. N. KRISHNAMURTHY, *J. Appl. Polym. Sci.* **1321** (1996) 60.
26. A. A. TAGER, *Vysokomol. Soed.* **19** (1977) 1654.
27. L. E. NIELSEN, in "Mechanical Properties of Polymers and Composities"(Marcel Dekker, Inc., New York, 1974) p. 310.
28. J. D. ANDRADE, L. M. SMITH and D. E. GREGONIS, in "Surface and Interfacial Aspects of Biomedical Polymers," edited by J.D. Andrade (Plenum Press, New York, 1985) Vol. 1, p. 249.
29. D. G. CASTNER and B. D. RATNER, *Surf. Sci.* **500** (2002) 28.
30. L. V. KARABANOVA, S. V. MIKHALOVSKY, L. M. SERGEEVA, S. T. MEIKLE, M. HELIAS and A. W. LLOYD, *Polym. Eng. Sci* **44** (2004) 940.
31. L. V. KARABANOVA, L. M. SERGEEVA, S. V. MIKHALOVSKY, J. SALVAGE, S. BUTLER and A. W. LLOYD, in Proceedings of the 9 International Conference "Polymers in Medicine and Surgery," Krems, Austria, September 2000, p. 13.